Microstructure Evolution in a 3%Co Modified P911 Heat Resistant Steel under Creep Conditions

Alla Kipelova[1,a], Rustam Kaibyshev[1,b], Andrey Belyakov[1,c] Izabella Schenkova[2,d] and Vladimir Skorobogatykh[2,e]

[1] Belgorod State University, Pobeda 85, Belgorod, 308015, Russia

[2] Central Research Institute for Machine-Building Technology, Sharikopodshipnikovskaya 4, Moscow, 115088, Russia

[a]kipelova@bsu.edu.ru, [b]rustam_kaibyshev@bsu.edu.ru, [c]belyakov@bsu.edu.ru, [d]in_material@mail.ru, [e]polyform_k@mail.ru

Keywords: Creep resistant steel; tempered martensite; dispersion strengthening; creep test; microstructure evolution.

Abstract. The microstructural changes in a 3%Co modified P911 heat resistant steel were examined under static annealing and creep at elevated temperatures. The quenched steel was tempered at temperatures ranging from 673 to 1073 K for 3 hours. The temperature dependence of hardness for the tempered samples exhibits the maximum at 723 – 823 K which is associated with the precipitations of fine carbides with an average size of about 20 nm. The transverse lath size of martensitic structure is ~ 200 nm after air quenching and remains unchanged under tempering at temperatures below 800 K. An increase in tempering temperature to 1073 K resulted in hardness drop. Coagulation of carbides and growth of martensitic laths takes place at these temperatures. The creep tests were carried out at 873 and 923 K up to rupture, which occurred after about 4.5×10^3 hours. The structural changes in crept specimens were characterized by the development of coarse laths/subgrains. The mean transverse size of which was ~ 0.67 and ~ 1.3 μm after the creep tests at 873 and 923 K, respectively. On the other hand, an average size of second phase particles of ~ 165 nm was observed in the samples tested at both temperatures.

Introduction

Recently, martensitic steels containing 9-12%Cr were implemented into commercial use as material of new generation for fossil power plants [1-6]. These steels are considered as promising structural materials for high temperature applications because of their improved creep resistance at elevated temperatures up to about 900 K. The beneficial combination of mechanical properties is achieved by a complex alloying to provide a solution strengthening along with precipitation strengthening associated with homogeneous distribution of stable second-phase nanoscale dispersoids. In addition, these dispersoids play a role of effective pinning agents preventing occurrence of recrystallization and recovery under creep conditions. As a result, the lath microstructure of tempered martensite is essentially stable against recrystallization and/or grain growth process, when the steels are in service. The creep resistance, therefore, depends on the stability of original tempered martensitic structures at elevated temperatures.

Further improvement of creep resistance of martensitic steels can be achieved through additional alloying. A possible effect of various alloying elements and their amounts on the service properties of 9-12%Cr martensitic steel at elevated temperatures is currently one of the most widely discussed topics [1, 3, 4]. The steels alloyed with about 4%Co were shown to exhibit superior creep strength [7, 8]. It is discussed that enhanced creep resistance of cobalt alloyed steels is mainly associated with an extra solution strengthening and a reduction of δ-ferrite. However, the effect of cobalt addition on the strength of martensitic creep resistant steel has not been studied in sufficient detail.

The aim of the present work is to examine the effect of temperature on microstructure evolution and precipitation behavior during tempering of a 3%Co modified P911-type martensitic steel. The study is also aimed on the structural changes and the coarsening of dispersed precipitates during long term creep tests.

Experimental Procedure

A cobalt bearing P911-type steel (C:0.11, Si:0.07, Cr:9.0, Co:2.9, Mo:0.9, W:1,1, V:0.17, Nb:0.07, N:0.04, B:0.005, all in mass%, and the balance Fe) was produced by Central Research Institute for Machine-Building Technology, Russia. The average prior austenite grain size was about 14 μm. The samples were austenitized at 1323 K for 0.5 h followed by air cooling and tempering at temperatures ranging from 673 to 1073 K for 3 hours. The samples for creep tests were tempered at 1023K for 3 h. Creep tests were carried out at 873 and 923 K up to rupture, which occurred in about 4.5×10^3 hours under starting stresses of 200 and 120 MPa, respectively. Specimens of 10 mm gauge diameter and 50 mm gauge length were used. Measurements of the transformation temperatures, such as A_{c1}, A_{c3} and M_s were conducted by differential scanning calorimetry, DSC (SDT Q600), on disk samples with a diameter of 5 mm and a thickness of 0.4 mm. The DSC samples were heated and cooled in Al_2O_3 crucibles with the rates of 2 and 20 K/min in an argon atmosphere. The crept microstructures were analysed on the longitudinal section (about 1.5 mm away from the fracture surface) with a reference to thread portions of samples. The microstructure of the steel was examined using a Quanta 600F scanning electron microscope equipped with a backscatter diffraction (EBSD) analyzer and a JEM-2100 transmission electron microscope (TEM) operating at 200 kV. The TEM foils were prepared by the double jet electro-polishing method using a 10% solution of perchloric acid in glacial acetic acid.

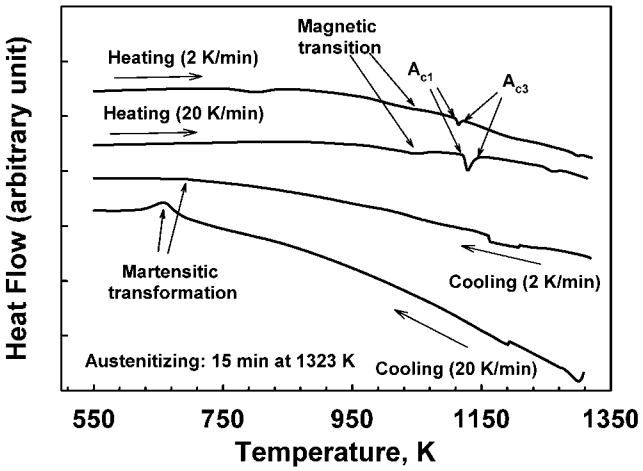

Fig. 1. DSC curves of a P911 + 3%Co steel, showing the transformation temperatures, such as A_{c1}, A_2, A_{c3}, M_s and M_f, on heating and on cooling.

Table 1.Transformation temperatures of a P911 + 3%Co steel [K].

	Heating and cooling rate of 2 [K/min]	Heating and cooling rate of 20 [K/min]
A_{c1}	1103	1114
A_2	1051	1050
A_{c3}	1134	1163
M_s	717	707
M_f	683	589

Results and Discussion

Differential Scanning Calorimetry. Fig. 1 shows the results of DSC obtained on heating and cooling with the rates of 2 and 20 K/min. Commonly, the changes in heat flow are more pronounced during the processing with higher heating/cooling rates. Two critical temperatures were recognized during the heating. Small broad endothermic peaks are observed with a peak temperature of about 1050 K during heating with the both rates. These peaks correspond to the magnetic transition from ferromagnetic to paramagnetic state. Then, remarkable endothermic peaks corresponding to the transformation from initial martensite to austenite are registered at temperature of about 1100 K. The DSC curve that obtained during cooling with the rate of 20 K/min exhibits a large exothermic peak resulting from the martensitic transformation

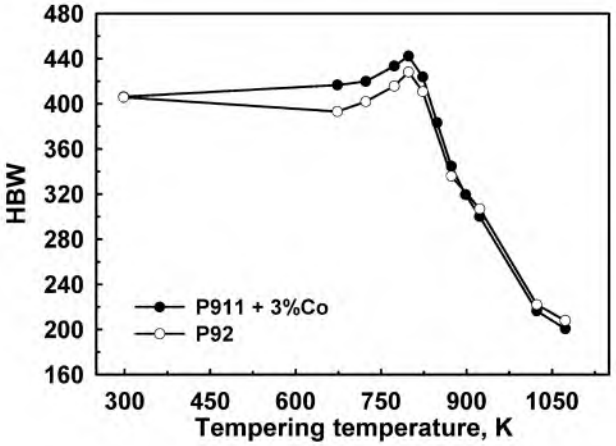

Fig. 2. Hardness change of a P911+3%Co and P92 steels after austenitizing at 1323 K for 0.5 h and tempering for 3 h at the temperatures between 673 and 1073 K.

below 707 K. Also, on cooling with the rate of 2 K/min, a weak exothermic reaction takes place at somewhat higher temperature. Table 1 summarizes the defined transformation temperatures for the studied P911 + 3%Co heat resistant steel. It should be noted that the A_{c1} and A_{c3} points are shifted to lower temperatures, while the M_s and M_f temperatures move to higher values, when the heating/cooling rates decrease.

Temperature Effect on Tempered Microstructures and Hardening. Variation of hardness for the tempered P911+3%Co steel with the tempering temperature is shown in Fig. 2. The figure also presents the hardness of P92-type steel tempered at the same temperatures for a reference. The hardness gradually increases from HBW405 in the initial state to HBW440 with increasing the tempering

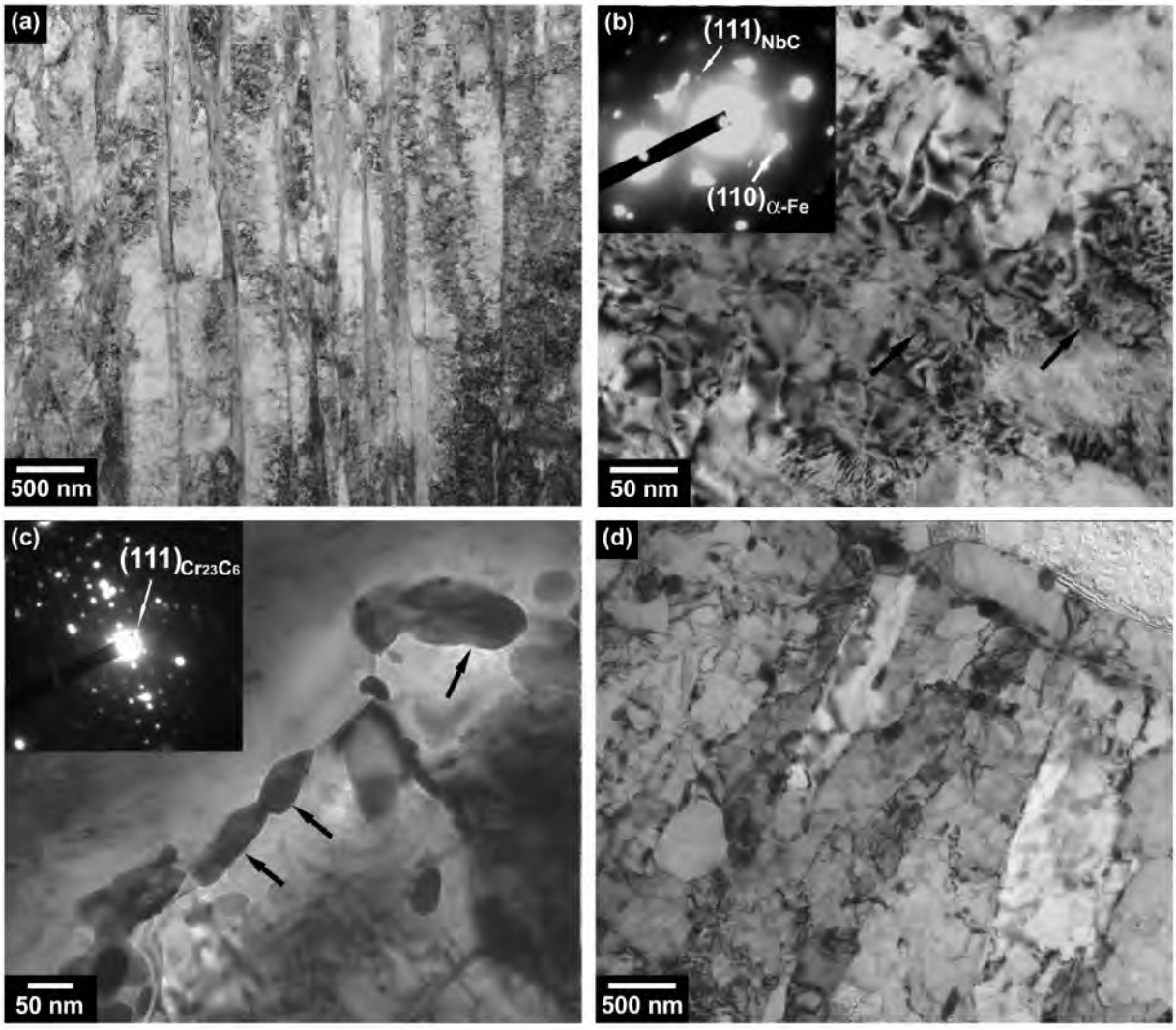

Fig. 3 Microstructure of the steel P911+3%Co after austenitizing at 1323 K for 0.5 h (a) and tempering for 3 h at 798 K (b), 898 K (c), 1023 K (d).

Table 2. Some microstructural parameters for P911 + 3%Co steel after different heat treatments.

Heat treatment	Mean transverse lath size [nm]	Dislocation density $\times 10^{14}$ [m^{-2}]	Mean carbide size [nm]
Austenitizing at 1323 K followed by air quenching	209	11.7	–
Tempering at 798 K	205	9.8	19
Tempering at 898 K	305	9.7	43
Tempering at 1023 K	368	6.2	82

temperature to 798 K followed by a rapid deterioration of strength after tempering at temperatures above 823 K. The samples of P92-type steel are characterized by a similar temperature dependence of hardness; however, the P911+3%Co steel samples demonstrate higher hardness after tempering at temperatures of 673 – 823 K.

Typical tempered microstructures developed in the P911+3%Co steel samples at various temperatures are shown in Fig. 3 along with the initial microstructure evolved by austenitizing treatment. The tempered microstructures consist of lath blocks with a fraction of special Σ3 boundaries of about 10pct. The quantitative results of tempered microstructures are collected in Table 2. Generally, the transverse size of martensite laths increases and the dislocation density in lath interiors decreases with increasing the tempering temperature. Tempering at 798 K (the hardness peak temperature in Fig. 2) does not change the lath size of about 210 nm, while the interior dislocation density slightly decreases form 1.2×10^{15} to 9.8×10^{14} m^{-2}. The hardening maximum is associated with fine carbide of NbC-type as suggested by TEM diffraction (s. Fig. 3b). These particles with an average size of about 20 nm are homogeneously distributed throughout the tempered martensite substructure.

Increase in the tempering temperatures leads to remarkable growth of martensite laths. The transverse lath sizes are about 300 and 370 nm after tempering at 898 and 1023 K, respectively. Correspondingly, relatively large second-phase particles precipitate in the tempered microstructures. The mean particle size ranges up to about 80 nm after tempering at 1023 K. It should be noted that the most of such large particles are carbides of $Cr_{23}C_6$-type, which precipitate mainly at lath and block boundaries (Fig. 3c and 3d).

Crept Microstructures. The P911+3%Co steel samples were subjected to creep tests after tempering at 1023 K. Typical microstructures evolved in the neck portion of samples after creep for about 4.5×10^3 hours are shown in Fig. 4. The creep tests resulted in significant changes of the microstructure of tempered martensite (*cf.* Fig. 3d and 4). The martensite substructures lose their lath morphology and look like an ordinary subgrains evolved by a hot working. The size of substructural elements after creep tests significantly exceeds the lath size in tempered martensite. Some microstructural parameters for the crept samples are presented in Table 3. The transverse subgrain sizes that develop in the neck portions are about 670 and 1300 nm in the samples tested at 873 and 923 K, respectively. The development of rather large subgrains in neck portions during the creep tests is accompanied with a remarkable coarsening of second-phase particles. The particles experience almost two-fold increase in their size.

On the other hand, the starting microstructure in the thread portions of crept specimens is less affected by the tests. The subgrain sizes in the thread portions are 0.51 and 0.56 μm after tests at 873 and 923 K, respectively. Also, the static annealing has negligibly small effect on the coarsening of second-phase particles. Almost the same mean particle size of 86 nm is evaluated in the thread portion of the sample tested at 873 K; and a little particle coarsening to about 120 nm is observed after creep at 923 K. Therefore, the remarkable structural changes in the neck portion of crept specimens are caused by plastic deformation. Decreasing the fraction of special Σ3 boundaries

during creep from about 0.1 to 0.03 in the neck portion argues for dynamic character of microstructure evolution as well. The subgrain size (d) and the dislocation densities (ρ) evolved in the neck portions are in rather fair correlation with the flow stresses, i.e. $\sigma \sim d^{-1} \sim \sqrt{\rho}$. The coarsening of second-phase particles is also accelerated by plastic flow, although the size relationship between grains/subgrains and particles is still unclear.

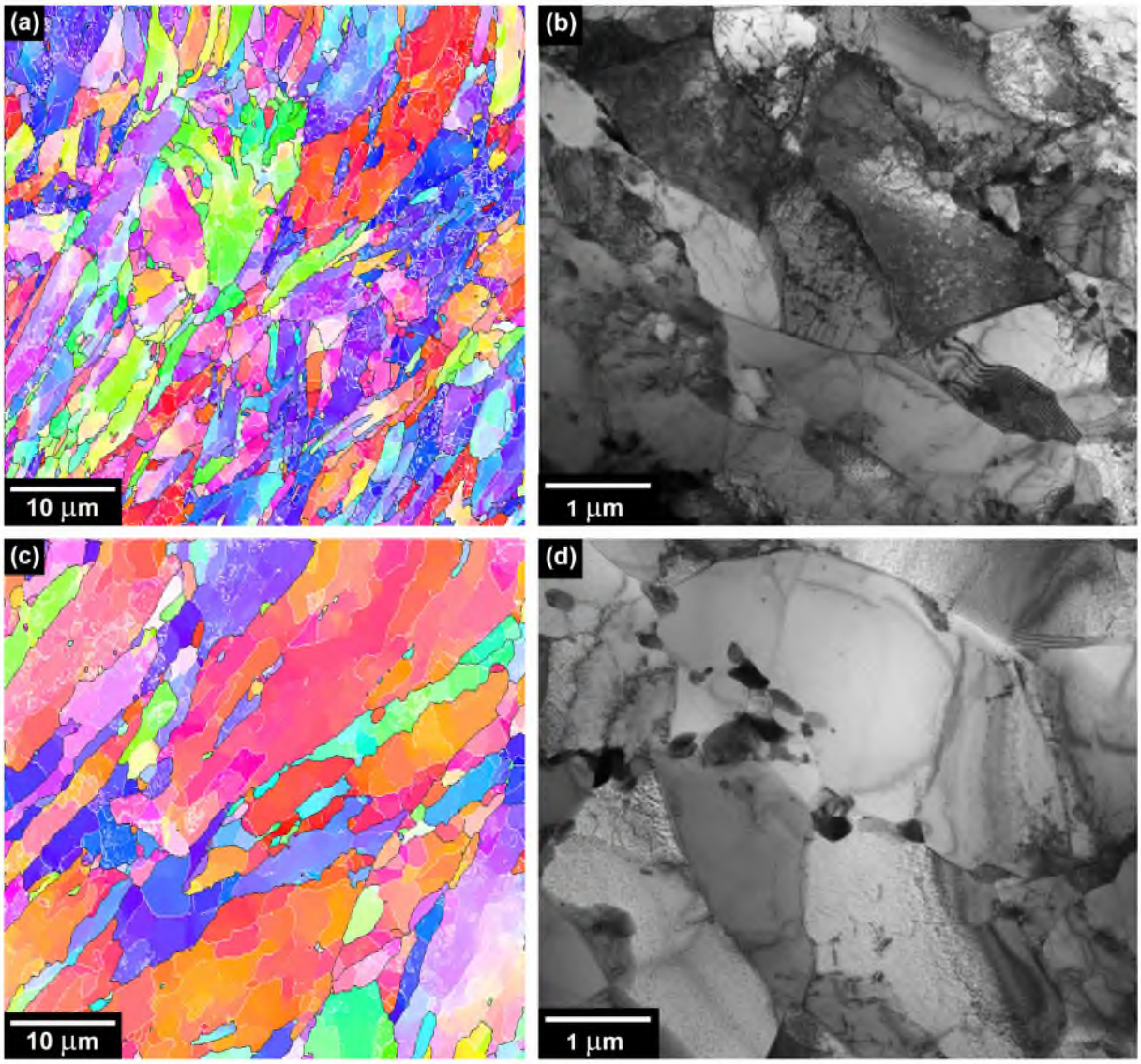

Fig. 4. EBSD maps and TEM images for neck portions of a P911+3%Co steel specimen after creep rupture testing at 873 K, 200 MPa (a, b) and 923 K, 120 MPa (c, d).

Table 3. Microstructural parameters for P911 + 3%Co steel after creep testing.

Creep test		Mean transverse lath/subgrain size [nm]	Dislocation density x 10^{14} [m^{-2}]	Mean phase size [nm]	Fraction of Σ3 boundaries
873 K/200 MPa/4103 h	neck portion	670	1.7	165	0.027
	thread	510	5.3	86	0.14
923 K/120 MPa/4743 h	neck portion	1300	0.46	165	0.032
	thread	560	2.86	126	0.073

Summary

The microstructure evolution in a P911+3%Co martensitic steel during tempering and creep was studied. A maximal hardening was achieved after tempering at a temperature of around 800 K. This increase in the hardness resulted from dispersion strengthening by a homogeneous precipitation of fine carbides with an average size of about 20 nm. The transverse lath size of about 200 nm after austenitization did not change by tempering at temperatures below 800 K. An increase of the tempering temperature to 1073 K resulted in remarkable softening that was caused by growing the both second-phase particles and martensite laths. The structural changes in the neck portions of crept specimens were characterized by a development of rather large subgrains in place of martensite laths. The transverse subgrain sizes were about 670 and 1300 nm in the samples crept at 873 and 923 K, respectively. The lath/subgrain growth was accompanied by two-fold increase in the size of second-phase particles.

Acknowledgements

The study was supported by Federal Agency for Science and Innovations, grant No. 02.523.12.3019. Authors are grateful to Mr. E. Kudryavtsev, Center of Common Facilities, Belgorod State University, for his assistance in specimens preparation and instrumental analysis.

References

[1] P.J. Ennis and A. Czyrska-Filemonowicz: Sadhana Vol. 28 (2003), p. 709.

[2] M. Taneike, F. Abe and K. Sawada: Nature Vol. 424 (2007), p. 294.

[3] F. Abe, M. Taneike, K. Sawada: Int. J. Pressure Vessels and Piping Vol. 84 (2007), p. 3.

[4] F. Abe: Int. J. Pressure Vessels and Piping Vol. 85 (2008), p. 99.

[5] J.C. Vaillant, B. Vandenberghe, B. Hahn, H. Heuser, C. Jochum: Int. J. Pressure Vessels and Piping Vol. 85 (2008), p. 38.

[6] T. Tokunaga, K. Hasegawa, F. Masuyama: Mater. Sci. Eng. A (2008), doi:10.1016/j.msea.2008.05.059.

[7] K. Yamada, M. Igarashi, S. Muneki and F. Abe: ISIJ Inter. Vol. 43 (2003), p. 1438.

[8] F.-S. Yin, W.-S. Jung: Metall. Mater. Trans. A Vol. 40 A (2009), p. 302.